Phytopathology

Peanut seed cultivars with contrasting resistance to A. parasiticus colonization display differential temporal response of protease inhibitors

Journal:	*Phytopathology*
Manuscript ID	PHYTO-09-16-0346-R
Manuscript Type:	Research
Date Submitted by the Author:	23-Sep-2016
Complete List of Authors:	Müller, Virginia; Universidad Nacional de Cordoba, Bioquimica Clinica-CIBICI Bonacci, Gustavo; Universidad Nacional de Cordoba, Bioquimica Clinica-CIBICI Batthyany, Carlos; Institut Pasteur Montevideo Amé, María; Universidad Nacional de Córdoba, Departamento de Bioquímica / CIBICI Carrari, Fernando; Instituto Nacional de Tecnologia Agropecuaria Gieco, Jorge; Instituto Nacional de Tecnologia Agropecuaria Asis, Ramon; Facultad de Ciencias Quimicas, Universidad Nacional de Cordoba, Bioquimica Clinica
Keywords:	Postharvest pathology and mycotoxins, Biochemistry and cell biology, Genetics and resistance

Peanut seed cultivars with contrasting resistance to *A. parasiticus* colonization display differential temporal response of protease inhibitors.

Müller, Virginia[a]; Bonacci, Gustavo[a], Batthyany, Carlos[b], Amé, MaríaV.[a]; Carrari, Fernando[c]; Gieco, Jorge[d]; Asis, Ramón[a].

[a] Departamento de Bioquímica / CIBICI, Facultad de Ciencias Químicas, Universidad Nacional de Córdoba, Haya de la Torre interseccion Medina Allende, Ciudad Universitaria, CP5000, Córdoba, Argentina.[b]Unidad de Bioquímica y Proteómica Analítica, Institut Pasteur de Montevideo. [c]Instituto de Biotecnología, Instituto Nacional de Tecnología Agropecuaria, Hurlingham, Buenos Aires, Argentina. [d] Instituto Nacional de Tecnología Agropecuaria, Estación Experimental Manfredi, Córdoba, Argentina.

Corresponding author: Ramon Asis; E-mail address: rasis@fcq.unc.edu.ar

ABSTRACT

Significant efforts are being made to minimize aflatoxin contamination in peanut seeds and one possible strategy is to understand and exploit the mechanisms of plant defense against fungal infection. In this study we have identified and characterized, at biochemical and molecular levels, plant protease inhibitors (PPIs) produced in peanut seeds of the resistant PI337394 and the susceptible Forman cultivar during *A. parasiticus* colonization. With chromatographic methods and 2D electrophoresis-mass

spectrometry we have isolated and identified four variants of Bowman-Birk trypsin inhibitor (BBTI) and a novel Kunitz-type protease inhibitor (KPI) produced in response to *A. parasiticus* colonization. KPI was detected only in the resistant cultivar while BBTI was produced in the resistant cultivar in a higher concentration than susceptible cultivar and with different isoforms. The kinetic expression of *KPI* and *BBTI* genes along with trypsin inhibitory activity was analyzed in both cultivars during infection. In the susceptible cultivar an early PPI activity response was associated with BBTI occurrence. Meanwhile in the resistant cultivar a later response with a larger increase in PPI activity was associated with BBTI and KPI occurrence. The biological significance of PPI in seed defense against fungal infection was analyzed and linked to inhibitory properties on enzymes released by the fungus during infection, and to the antifungal effect of KPI.

INTRODUCTION

Plant protease inhibitors (PPIs) are important elements of the plant defense machinery against insects, nematodes and phytopathogenic microorganisms. In insects and nematodes, PPIs inhibits the enzyme activity of the digestive tract and suppresses the normal assimilation of food proteins. In phytopathogenic microorganisms, the defense role of PPIs is attributed to the inhibition of the secreted proteases necessary for entering plant cells and supplying the pathogen with nutrients (reviewed by Mosolovand Valueva 2005; Hörgerand van der Hoorn 2013; Yarullina et al. 2016). In addition, members of PPI family have shown anti-microbial activity such as cysteine protease inhibitor of sunflower seeds, millet and snuff against *Fusarium* and

Trichoderma (Kouzuma et al. 2000; Joshi et al. 1998; Park et al. 2000) or different maize protease inhibitors against several pathogens (Roberts et al. 1990; Chen et al. 1999; Carrillo et al. 2011).

Peanut seeds as hypogeous fruits are in direct contact with soil fungal populations, and are frequently colonized by mycotoxigenic fungi such as *Aspergillus flavus* and *Aspergillus parasiticus*. Success of seed colonization depends on the fungus skill to pass through the outer barrier and exploit the nutrients from the seeds. In a previous report, we have proposed that protease production by *A. parasiticus* is related to infection and aflatoxin contamination in peanuts. This contributes to generating tissue damage affecting seed viability and germination, providing access to fungus invasion through the integument (Asis et al. 2009). The use of enzymes as tools to degrade physical barriers by various pathogenic fungi is directly related to the production of proteolytic enzymes (Vernekar and Deshpande 1999; Chen et al. 2009). Serine and metallo proteases were described as the main fungal extracellular proteases produced by *A. flavus and A. parasiticus* during colonization of peanut seed (Asis et al. 2009).

Given the role of fungal proteases during seed colonization, seed protease inhibitors would be important pieces in the defense against aflatoxin-producing *Aspergillus*. Differential gene expression studies with peanut seeds in response to *A. parasiticus* infection have reported an increase in protease inhibitor gene expression after fungal inoculation (Guo et al. 2008; Luo et al. 2005). However, the role of these proteins in peanut seed defense is still not clearly understood. The aim of this research was to identify PPIs from peanut seed in response to *A. parasiticus* challenge and to explore their role in seed defense and fungal colonization resistance. Here, we report

the identification and characterization of two PPIs and their gene expression patterns in peanut seeds from two cultivars with contrasting behavior against *A. parasiticus* infection, by applying proteomic tools and real-time PCR. Additionally, different functions of both PPIs in seed defense were discussed.

MATERIAL AND METHODS

Plant material. Peanut seeds of the two cultivars were provided by the Instituto Nacional de Tecnología Agropecuaria (INTA, Manfredi Experimental Station, Córdoba, Argentina). The PI337394 cultivar was previously characterized as resistant and the Florman INTA cultivar as susceptible to *Aspergillus spp.* infection (Asis et al. 2005).

Seed samples of tested cultivars were obtained from the same growing season (2010-2011). The cultivars were planted in a two-row plot of 10 m long, with an inter-row distance of 0.70 m at 1 seed/20 cm linear row, in a completely randomized block design with two replicates. In turn, to eliminate all weed, preplant (Imazetapir 100 cm3 of ai/ha) and postemergence (Cletodin 175 cm3 of ai/ha) herbicides were used. Leaf spot was avoided using contact fungicide (Mancozeb 1 kg of ai/ha). Two complementary irrigations (50 mm) were carried out in February and March to avoid drought stress. Each cultivar was manually harvested at its optimum maturity and threshed. Harvested pods, naturally dried to 5.5% moisture, were hand-sorted to remove and discard visibly damaged pods and stored in bags in a seed chamber at 7°C until use. Pods were hand-shelled before performing the experiments.

***Aspergillus spp.* source.** Isolate #18 of *Aspergillus parasiticus* was used for all the experiments reported here. This isolate was previously determined as highly

aflatoxigenic and infective in peanut seeds (Asis et al. 2005). The fungi were grown on potato-dextrose agar (PDA) (Merck) at 30°C for 7 days. Spore suspensions were obtained by washing the surface of the cultures with Tween 80 (0.5 ml/L) and quantified in a Neubauer chamber.

Infection assay and seed treatment. For all experiments, seeds without tegument of both cultivars (PI337394 and Florman INTA) were surface-sterilized with sodium hypochlorite. Disinfected seeds were inoculated with 1 ml of spore suspension of *A. parasiticus* (1 x 10^4 spores/ml) and incubated at 30°C in Petri dishes. Control seeds received an equal amount of Tween 80 (mock inoculated). For PPIs purification, seeds were incubated for 48 h.

For gene expression analysis, three independent biological replicates were conducted in parallel and samples were collected at 5-h, 10-h, 20-h, 27-h, 48-h and 72-h after inoculation (a.i.).

In each sample collected, seeds were examined by visual inspection to identify the presence or absence of mycelium; the percentage of colonized seed was then calculated.

PPIs extraction and acetone precipitation. Seeds were lyophilized for 16-h and then ground and defatted with chilled hexane (-20°C) using an Ultraturrax T18 basic (IKA Works Inc.). Defatted meals were used to extract PPIs with a solution of glacial acetic acid (0.05M) 1:10 w/v using Ultraturrax T18. The homogenate was centrifuged at 10,000 rpm for 10 min at 4°C. Subsequently proteins were precipitated twice by acetone fractionation with addition of cold acetone at 30% v/v and 70 % v/v, consecutively,

overnight at -20°C. Samples were then centrifuged at 13,000 rpm for 10 min at 4 °C and resuspended in buffer 20 mM Tris-HCl (pH 6.4).

PPIs purification. PPIs were isolated by Ion Exchange Chromatography using a Fast Protein Liquid Chromatography (FPLC) equipment (Amersham Bioscience). The PPIs extract was loaded on a Mono Q HR 5/5 (1 ml) column equilibrated with 30 ml of 20 mM Tris-HCl (pH 7.5), solution A. The column was washed with 10 ml of solution A and protein elution was performed with a linear gradient of 0-100% 0.5M NaCl in solution A. The flow rate was 60 ml/h and the absorbance of eluates was monitored at 280 nm.

The fractions collected in the void volume of the ion exchange chromatography were subjected to a second step of chromatographic separation through a molecular filtration. For that purpose, a Bio-Gel P-(Bio-Rad) was used. The separation was performed with 50 mM Tris-HCl (pH 6.8)/200 mM NaCl at a flow rate of 15 ml/h.

In both chromatographic analyses, fractions of 0.5 ml were collected and their trypsin inhibitory was activity evaluated.

Two-dimensional gel electrophoresis. Proteins of selected fractions of anionic and gel permeation chromatography were precipitated with acetone 70%, resuspended in a 20 mM Tris-HCl buffer (pH 8.9) solution and treated with the kit (2-D Clean-up kit, Amersham Biosciences) to remove interfering substances. The first dimension analysis was performed with isoelectric focusing Ettan IPGphor 3 (Amersham Biosciences) using IPG strips (pH 3-10, 7 cm). IPG strips were rehydrated with sample solution (0.125 ml) in the rehydration IPG box (Amersham Biosciences) for 10-24 h at room temperature. Strips were then covered with mineral oil (fluid cover, Amersham Biosciences) and run in four steps with 6299 Vh at 20 °C. They were removed and incubated for 15 min with a

50 mM Tris-HCl buffer (pH 8.8) solution containing 6M urea; 30% (v/v) Glycerol; 2% (w/v) SDS; 1% (v/v) DTT; 0.002% (w/v) bromophenol blue. The solution was then removed and replaced with another one containing the same components, except that DTT was replaced by 4% (w/v) iodoacetamide. The strips were positioned on a SDS-PAGE gel at 16% and proceeded to run at a constant current of 50 mA. The stacking gel was prepared at 4% (w/v) acrylamide in 0.5 M Tris-HCl (pH 6.8) solution while resolving gel was prepared at 16% (w/v) of acrylamide in 1.5 M Tris-HCl (pH 8.8). Electrophoretic analysis was performed with a constant current of 30 mA at 4 °C on a Mini Protean III electrophoresis cell (Bio-Rad Laboratories), using electrophoresis solution: 0.1M Tris-HCl (pH 8.3); 0.1M tricine; 0.1% (w/v) SDS (sodium lauryl sulfate) (Schägger 2006).

Proteins were detected by staining with Coomassie Brilliant Blue R250 and molecular weight was calculated from a calibration curve with commercial molecular weight marker protein (log MW vs. relative mobility) (Bio-Rad).

Identification of 2D gel protein spots by *MALDI-TOF/TOF.* Proteins of excised gel plugs were digested with trypsin for 16 h (Promega, sequencing grade). Peptides were extracted from gel with a solution of 60% (v/v) acetonitrile with 0.2% (v/v) trifluoroacetic acid, concentrated by vacuum drying and desalted using C18 (Omix, Varian). Eluted peptides were injected directly into the mass spectrometer with 3 µl of matrix solution (α-cyano-4-hydroxycinnamic acid in 60% (v/v) acetonitrile with 0.2% (v/v) trifluoroacetic acid acid). The mass spectrum of the digested samples was performed on a MALDI-TOF/TOF (Biosystems) mode and reflector equipment externally calibrated with a mixture of peptide standards (Biosystems). Proteins were identified with NCBI nr

database using search with the values of m/z and MASCOT program with the following pre-selected parameters: mono isotopic mass tolerance 0.05 Da; fragment mass tolerance of 0.25 Da; methionine oxidation and tryptic cleavage as fixed modifications.

Trypsin inhibitory assay. The inhibitory activity was determined spectrophotometrically using 0.1 % (w/v) of benzoyl-α-arginine p-nitroaniline (Sigma) as substrate. An aliquot of 47 µl of eluted fractions was mixed with 233 µl of substrate, 47 µl of trypsin (1000 u/ml in 1 mM HCl, Sigma) and buffer triethanolamine/20mM CaCl2 (pH 7.8) up to 1 ml final volume. The absorbance was scanned at 405 nm, every 1 s (during 5 m) at 25 °C in a Shimadzu UV1601 spectrophotometer. One trypsin inhibitory unit (TIU) will decrease the activity of two trypsin units by 50 % where one trypsin unit will hydrolyze 1 µmol benzoyl-α-arginine p-nitroaniline per minute at pH 7.8 at 25 ºC. TIU: (Δ Abs/min of uninhibited control – Δ Abs/min of sample) / 9.96 (mM^{-1} * cm^{-1} EC p-nitroaniline) * (ml sample / ml reaction mix).

PPI activity in reverse zymography. SDS-PAGE gel at 16% was performed as described in second-dimension electrophoresis, with the addition of 0.1% (w/v) casein in the polymerization of acrylamide. The electrophoretic run was performed at 100 V at 4 °C on a Mini Protean III electrophoresis cell (Bio-Rad Laboratories), using electrophoresis solution: 0.1 M Tris-HCl (pH 8.3); 0.1M tricine; 0.1% (w/v) SDS. The PPI samples were loaded onto the gels in a sample buffer containing 10% (w/v) glycerol, 0.001% (w/v) bromophenol blue and 20 mM dithiothreitol without heating to avoid loss of activity. After electrophoresis, the gel was incubated for 1 h in a solution of 2.5% (w/v) Triton X-100 to remove the SDS.

After 1 hour, all lines except that containing molecular weight markers were placed in a 0.01% (w/v) trypsin (Trypsin 250 BD Difco) solution in 10 mMTris-HCl (pH 7), 200 mM NaCl and 10 mM CaCl2 and incubated at 37 °C for 8 h. Following proteolysis, the gels were stained with Coomassie Brilliant Blue R250 125 mg% in methanol solution 40% v/v acetic acid and 10% v/v. Then gel destaining was performed with a solution of 5% methanol and 10% acetic acid.

Fungal protease inhibition in Zymography study. In the zymography test the enzymes were separated by electrophoresis and detected by their ability to hydrolyze casein in the migration region according to Asis et al. (2009). *A. parasiticus* was incubated in casein liquid medium at 30°C for 10 days. The culture medium was filtered and the extracellular proteases were precipitated from the filtered culture medium by the addition of -20°C cold acetone (80% of total volume). The precipitate was dissolved in 50 mM phosphate buffer (pH 7). The enzyme extracts were diluted (1/4) in sample buffer containing SDS without reducing agents and not boiled before loading onto the gels. Electrophoresis was carried out using 10% acrylamide co-polymerized with 1 g/L sodium casein (Sigma-Aldrich) in a vertical electrophoresis system Miniprotean (Bio-Rad) at a constant voltage of 100 V in an ice bath. After electrophoresis, the gel was washed with Triton X-100 and incubated for 48 h at 37°C in an enzyme buffer (50 mM Tris-HCl (pH 7.5), 200 mM NaCl, and 1.8 mM CaCl2) with the presence or absence of inhibitor (control). After incubation, the gels were stained with 5 g/L Coomassie Brilliant Blue G250 in 30% (v/v) methanol and 10% (v/v) acetic acid. The unstained regions showed protease migration in the gels. Protease activity in the gels was estimated by densitometric analysis using Image J software. To inhibit the four classical protease

groups: metallo, serine, cysteine and aspartic protease, 10 mM EDTA, 5 mM PMSF, 100 µM iodoacetamide and 1 mM pepstatin were used, respectively.

Antifungal assay. For the antifungal assay, an aliquot of eluted fraction (0.010 ml) was incubated with a 90 µl of *A. parasiticus* suspension (1 x10^4 spores/ml) in Mueller Hinton liquid medium with chloramphenicol (0.045 ml/50 ml) at 37 °C for 24 h. After the incubation period the absorbance at 600 nm was determined to express the development of fungal mycelium, confirmed by microscopic observation.

Gene expression analyses. q RT PCR was performed according to Muller et al. (2015). In brief, Total RNA was extracted from frozen seeds with the plant RNeasy kit (Qiagen) and RNA samples were treated with DNase I (Fermentas) to remove contaminating DNA. A quantity (1 µg) of this RNA was used to prepare cDNA using Revert Aid M-MuLV Reverse Transcriptase (Fermentas). Gene expression was quantified by qRT–PCR analyses using a Bio-Rad iQ cycler with 1 µL of a dilution of cDNA (50 ng reverse-transcribed total RNA), SYBR Green PCR Master Mix spiked with fluorescein 10 nM (Applied Biosystems) and 0.3 µM primers in a final volume of 15 µL. Primers were designed by using the Primer Express TM (Applied Biosystems) software based on sequences deposited in the Gene bank under the following accession numbers: AY330200.1 and ES761053. Primer information on each gene is shown in supplementary Table 1. Gene-specific PCR amplification efficiency was calculated using the following equation: efficiency % = (10^(-1/slope) - 1) × 100. Histone H3 encoding gene (*H3*) was used as a reference gene according to expression stability for normalization of gene expression.

Statistical analyses. Statistical analyses were carried out using the Infostat Software Package (Infostat, 2002). All values are expressed as means ± standard deviation. All data were subjected to Analysis of Variance (ANOVA). When significant differences were found by ANOVA, the Fisher test was used to compare treatments. When not normally distributed, data were subjected to nonparametric statistical analysis on ranks (Kruskal–Wallis) followed by Dunn's post-test. Significance was accepted at $P < 0.05$ for all comparisons.

RESULTS

PPI purification and identification. In order to identify proteins with protease inhibitory activity in peanut seeds during fungal infection, we inoculated with *A. parasiticus* spores two cultivars with contrasting behavior in relation to this fungus: Florman (susceptible) and PI337394 (resistant). The external seed infection was measured by visual inspection after 48 h of incubation at 30 °C (Supplementary Fig. S1). The percentage of colonized seeds was 90 ± 7 and 6 ± 3 % of total infected seeds in the susceptible and resistant cultivar, respectively.

To explore whether the differences in fungal colonization are related to protease inhibitor expression, PPIs were extracted from defatted meals of infected and control seeds (mock inoculated). Subsequently PPIs were isolated by cold acetone fractionation where the main PPI activity was detected at 70% of acetone fraction (Table 1). PPI activity was higher in fractions derived from infected seeds when compared against those derived from control seeds. These PPIs were then purified by anion exchange chromatography (AEC) (Fig. 1A). In order to detect PPI activity the fractions

eluted were collected and subjected to trypsin inhibitory activity assay (Fig. 1B) and reverse zymography (Fig. 1C). The main PPI activity was detected in the fraction 1, 2 and 3 (AEC 1-3), corresponding to unbound proteins, and in the fraction 17, 18 and 19 eluted at 8 to 10 % of solvent B (AEC 17-19) (Fig. 1A and 1B). The reverse zymography assay of fraction 17, 18 and 19 exhibited PPI activity at molecular weight between 16.9 and 14.4 kDa (Fig. 1C). In both assays the fraction AEC 17-19 of resistant cultivar showed higher PPI activity compared to the susceptible cultivar (Figs. 1B and 1C).

Fractions AEC 1-3 were pooled and separated by gel permeation chromatography (GPC) as shown in the chromatogram of Fig. 2A. The main trypsin inhibitory activity was detected in the fractions 14, 15 and 16 (GPC 14-16) (Fig. 2B). In these fractions, reverse zymography analysis exhibited PPI activity between 6.5 and 14.4 kDa (Fig. 2C). In both PPI assays (Figs. 2B and 2C), GPC 14-16 fraction of resistant cultivar showed higher PPI activity than the susceptible cultivar.

To identify these proteins, fractions AEC 17-19 and GPC 14-16 corresponding to resistant and susceptible cultivar were separated by 2D-SDS-PAGE (Figs. 3 and 4) and all spots were subsequently analyzed by MALDI-TOF. Peptide sequences were compared against NCBI data base nr (Non redundant protein sequences) and NCBI Peanut EST database. A total of 18 proteins were identified from the AEC 17-19 fraction of both cultivars (Figs. 3A and 3B). These protein profiles changed markedly between cultivars and most of these proteins were exhibited in the resistant cultivar (PI337394). The identified proteins are listed in Table 2. Only the protein Cu-Zn-super oxide dismutase could be found in both cultivars, while the remaining proteins were specific to each cultivar. Among the proteins identified in the resistant cultivar, we could find

proteins related to: metabolism (16 kDa malate dehydrogenase, triose phosphate isomerase, transaldose), stress (glutathione transferase, lactoyl glutathione lyase, glyoxalase, glutaredoxin, Cu-Zn-super oxide dismutase, allergen Ara h8) and protease inhibitory activity (Kunitz-type protease inhibitor) (Fig. 3A and Table 2). In contrast, in the susceptible cultivar different proteins related to metabolism (22 kDa malate dehydrogenase) and to stress (mannose binding lectin, galactose-binding lectin and Cu-Zn-super oxide dismutase) were found, whereas no protease inhibitors were detected (Fig. 3B and Table 2).

Two-dimensional gel electrophoresis of GPC 14-16 fractions from PI337394 and Florman cultivars are shown in Figs. 4A and 4B respectively. Thirteen protein spots were identified in these gels (Table 3). Proteins related to: stress (Cu-Zn-super oxide dismutase and pathogenesis-related protein class IV) and protease inhibitor activity (Bowman-Birk type inhibitor (BBTI): AI, BI and BIII isoforms) were found in both cultivars. However, other proteins were specific to PI 337394 cultivar such as those related to stress (BBTI AII isoform, allergen Arah 8, and glutaredoxin) and to protein modification (ubiquitin), while a galactose-binding lectin was found only in the Florman cultivar (Table 3). The densitometry analysis of BBTI isoforms found in both cultivars showed higher levels of these inhibitors in the resistant cultivars (PI337394, spot area of BIII: 6100, BI: 4600 and AI: 4000; Florman, spot area of BIII: 4700, BI: 3800 and AI: 3200).

Sequence and Phylogenetic Analyses. Considering the results from 2D-SDS-PAGE, the PPI activity observed in fractions AEC 17-19 is mainly based on the presence of Kunitz protease inhibitor (KPI) encoded by peanut EST ES761053 (Table

2). The product of this gene is a protein with a conserved Kunitz inhibitor domain, which has not been previously described (Supplementary Fig. S2). To characterize this Kunitz inhibitor protein, a phylogenetic analysis with other plant Kunitz inhibitors (Supplementary Fig. S3A) was performed. Phylogenetic tree clustered peanut KPI with soybean Kunitz inhibitor (MER017895), two inhibitors of *Erythrina variegate* (MER017915 and MER019771) and an inhibitor of *Psophocarpus tetragonolobus* (MER017908). The alignment of these sequences allowed identifying the common regions of Kunitz inhibitors: the characteristic cysteine residues and the active site consisting of lysine, leucine or arginine residue (Supplementary Fig. S4A).

Likewise, a phylogenetic tree was made for Bowman-Birk Trypsin inhibitors (BBTI) of peanut seeds by comparing its sequence with other plant BBTI from the Merops database (http://merops.sanger.ac.uk/) (Supplementary Fig. S3B). These BBTI were clustered with MER018102 and MER018107-*Arachis hypogaea* BBTI and the sequence alignment shows that BBTI identified here correspond to the BBTI isoforms previously reported in peanut seed (Norioka et al. 1983) (Supplementary Fig. 4B). These peanut BBTI isoforms were also related to BBTI of *Medicago* (MER025297 and MER024101-*Medicago sativa*, MER080341-*Medicago truncatula*), *Lens* (MER050434-*Lens culinaris*, MER055331-*Lens ervoides*, MER055333-*Lens nigricans*) and *Coptisjaponica* (MER078534). The sequence alignments of BBTIs show two reactive sites formed by an arginine or leucine residue capable of binding to the active site of serine proteases (Birk 1985) (Supplementary Fig. S4B).

Antifungal activity. In order to evaluate the ability of peanut seed PPIs to inhibit fungal growth, an antifungal assay was performed. *A. parasiticus* was grown in Mueller Hinton medium in the presence of AEC 17-19 fraction from resistant cultivar (containing KTI). After 24 h of incubation, fungal growth was determined by microscopic visualization and compared to that in mock-inoculated control. This assay showed a potent inhibitory effect of this protein fraction on the spore germination of *A. parasiticus* (Fig. 5). When GPC 14-16 fraction containing BBTI was tested, no antifungal activity was detected in both cultivars (Supplementary Fig. S5). Incubation with GPC 14-16 fraction of susceptible cultivar displayed a fungal growth higher than that in resistant cultivar fraction, showing an inductive effect on fungal growth (Supplementary Fig. S5).

Inhibitory assay of *A parasiticus* extracellular proteases. To assess the ability of peanut seeds PPI to inhibit *A. parasiticus* proteases, a zymography was performed in the presence of 70% acetone fraction from resistant cultivar (containing KTI and BBTI isoforms), a commercial inhibitor mix, and mock-inoculated control (Fig. 6). The control showed two main bands corresponding to 91 kDa serine-protease and 43.5 kDa metallo-protease previously reported for *A. parasiticus* (Asis et al. 2009). The protease activity measured by densitometry showed a reduction of 82% and 90 % of total activity with respect to control, when incubated with commercial inhibitor mix and peanut seed protease inhibitors, respectively. These results reveal the strong inhibitory activity of peanut seed PPIs against those proteases that contribute to *A. parasiticus* virulence.

PPI activity and Gene expression during *A. parasiticus* colonization. In order to evaluate the relationship between fungal infection response and PPIs, we

measured the PPI activity as Trypsin inhibitory units (TIU) in a time series of infected and mock-inoculated control peanut seeds. Different patterns of seed colonization and fold change TIU activity (infected vs control) were observed between cultivars along different infection periods (Fig. 7A and 7B, respectively). Infected and control seeds of Florman cultivar showed 60 and 4 % of seeds visually colonized by *A. parasiticus*, at 48 h of infection, respectively. Unlike Florman cultivar, infected and control seeds of PI337394 cultivar did not show colonization at any evaluated infection time (Fig. 7A). Infected Florman seeds showed a two-fold increase of TIU with respect to that in control seeds at 5 h a.i. Unlike that, infected seeds from PI337394 exhibited a 5-fold increase in TIU activity at 48 h a.i. (Fig. 7B).

To evaluate gene expression of *BBTI* and *KPI*, primers were designed from gene sequences (AY330200.1 and DQ889567.1, Supplementary Table 1) encoding PPI proteins identified in the two-dimensional electrophoresis (Table 1). Gene expression was assessed in peanut seeds at different infection times with *A. parasiticus* and was expressed as fold changes in relation to that in mock-inoculated control seeds (Fig. 7C and 7D). Different expression patterns for *BBTI* gene were observed between cultivars (Fig. 7C). The expression of *BBTI* in PI337394 cultivar was significantly up-regulated at 20 h a.i., followed by a strong down-regulation up to 48 h a.i. in response to fungal infection. By contrast, fold change analysis of *BBTI* in Florman did not display significant changes up to 27 h a.i. followed by a strong down-regulation at 48 h a.i. with respect to control seeds.

The expression of *KPI* showed differences in relation to *BBTI* expression and between both cultivars (Fig. 7D). In PI337394, *KPI* exhibited an up-regulation at 5, 10

and 27 h a.i and a strong down-regulation at 48 h a.i. in response to fungal infection. By contrast, in Florman cultivar *KPI* expression showed a strong down-regulation from 27 to 48 h a.i. in response to fungal infection.

DISCUSSION

Plant protease inhibitors (PPIs) are low molecular weight proteins which occur in several physiological processes and in response to different stresses (reviewed by Mosolov and Valueva 2005; Hörger and van der Hoorn 2013; Yarullina et al. 2016). In this study we have identified and characterized, at biochemical and molecular levels, protease inhibitors produced in peanut seeds during *A. parasiticus* colonization. To evaluate the regulation and participation of PPIs in seed defense, we have proposed to work with a model of two cultivars distinguished as resistant (PI 337394) and susceptible (Florman INTA) to *Aspergillus spp.* infection and aflatoxin contamination (Asis et al. 2005). We isolated by chromatographic and electrophoretic methods two protease inhibitors, which occurred in the resistant and susceptible cultivar in response to *A. parasiticus* colonization (Figs. 3 and 4). One protease inhibitor was identified as a Bowman-Birk type trypsin inhibitor (BBTI) previously reported and characterized in peanut seed (Norioka et al. 1983). The other was identified as a Kunitz-type protease inhibitor (KPI), which to our knowledge, has not been previously reported. The KPI sequence is closer to Fabaceae Kunitz-type protease inhibitor of *Glycine max* (MER017895), *Erythrina variegate* (MER017915 and MER019771) and *Psophocarpus tetragonolobus* (MER017908) (Supplementary Fig. S3A).

The occurrence of KPI and BBTI at 48 h after *A. parasiticus* inoculation was noticeably different between cultivars (Figs. 3 and 4, respectively). KPI was detected only in the resistant cultivar (Fig. 3), while BBTI isoforms were produced in a higher concentration, showing an extra isoform (BBTI AII) as compared with that in the susceptible cultivar (Fig. 4). These results agree with those of previous studies where protease inhibitor genes of peanut seed were differentially expressed between resistant (GT-C20 and A13) and susceptible (Tifrunner) cultivars in response to *A. parasiticus* infection (Luo et al. 2005; Guo et al. 2008). Within this gene group, BBTI, cysteine proteinase inhibitor and KPI (different from KPI reported here) were found over expressed in the resistant cultivars. In another study, protease inhibitors containing cupin domain were down-regulated in response to infection of toxigenic and non-toxigenic *A. flavus* strains in a susceptible peanut cultivar (Luhua 14) (Wang et al. 2012). All these results evidence a protease inhibitor participation in response to *Aspergillus* spp infection; this response being dependent on peanut genotype rather than on *Aspergillus* species or their aflatoxigenic capacity.

We have previously reported that the involvement of extracellular proteases of *A. parasiticus* in the fungal colonization of peanut seed affected seed viability, inducing tissue necrosis and promoting fungal colonization and aflatoxin production (Asis et al. 2009). On the basis of this study, we assessed the ability of protease inhibitors to modulate the activity of *A. parasiticus* extracellular proteases. Our results indicated a marked inhibitory effect on *A. parasiticus* protease activity (Fig. 6). These finding suggest that peanut protease inhibitors can be involved in the seed defense reducing the action of fungal proteases.

Another mechanism involving certain PPIs in plant defense is their antimicrobial capacity. When we evaluated the antifungal activity of chromatographic fractions containing BBTI, they did not show antifungal activity against *A. parasiticus*. In contrast, chromatographic fractions containing KPI displayed a strong antifungal activity against *A parasiticus*. Because of this fraction is composed of several proteins (Table 2), it is difficult to ascribe antifungal activity to KPI. However, several studies have shown that Kunitz inhibitors produce insecticide or antifeedant activity and also antifungal activity against plant pathogenic fungi. An example of this is the soybean Kunitz inhibitor closer in homology to peanut KPI (Supplementary Fig. S3A and S4A) which has the ability to inhibit *Fusarium oxysporum* (Wang et al. 2006). Another inhibitor is the *Acacia plumose* Kunitz inhibitor, highly homologous to *Acacia confuse* Kunitz inhibitor, that showed antifungal activity against *Aspergillus niger*, *Colletotrichum* sp. and *Fusarium moniliforme* (Lopez et al. 2009).

To examine the genetic response of protease inhibitors to *A. parasiticus* infection, expression of *KPI* and *BBTI* genes along with trypsin inhibitory activity was analyzed in infected and control seeds of both cultivars at post-infection time references. The results showed a differential temporal response between cultivars. In the seed of resistant cultivar, the trypsin inhibitory activity was increased at 48 h a.i. (Fig. 7B) and the expression of *KPI* and *BBTI* gene was moderately up-regulated from 5 to 27 h a.i., and 20 h a.i. respectively (Fig. 7C and 7D). Gene expression analyses showed that expression of both protease inhibitors would be contributing to the increase of trypsin inhibitory activity described in the resistant cultivar. In contrast, the trypsin inhibitory activity in the susceptible cultivar was slightly increased in the early hours of

infection (Fig. 7B). However, in this cultivar *KPI* and *BBTI* gene expression did not show significant changes between infected and control seeds at earlier times of infection (Fig. 7C and 7D). In this cultivar, only the presence of BBTI isoforms was detected at 48 h a.i. (Tables 2 and 3) and it is likely that overexpression of *BBTI* gene at earlier times had contributed to increasing trypsin inhibitory activity. Five BBTI Isoforms have been previously described in peanut seed (Norioka et al. 1983). The high identity of four of them (BIII, BI, AI and AII isoforms) suggests that they are code for same gene and isoforms originate from post-translational cleavage, while the remaining isoforms (BII isoform) derive from an unknown gene (Boateng et al. 2005). Considering the differences in BBTI isoform composition and gene expression between cultivars, BBTI response to fungal infection was differentially regulated at transcriptional and post-transcriptional levels between cultivars.

In conclusion, two types of PPIs that occurred during *A parasiticus* infection were identified as Kunitz-type inhibitor and BBTI isoforms AI, AII, BI and BIII. The results of this study showed a different temporal response of PPIs in seeds of two peanut cultivars challenged by *A. parasiticus* infection. In the susceptible cultivar an early PPI activity response, mainly associated with BBTI occurrence, was observed. Meanwhile in the resistant cultivar a later response with a larger increase in PPI activity was described as being associated with BBTI and KPI occurrence. The participation of these compounds in seed defense against fungal infection would be caused by the action of inhibiting extracellular enzymes that release the fungus during infection and by the antifungal effect of KPI produced by an unknown mechanism.

In the light of the results reported, it can be considered that *Aspergillus spp.* resistance in peanut seed is closely related to PPIs occurrence and to a novel Kunitz-type trypsin inhibitor. A genetic regulation of PPIs was clearly evidenced in the resistant cultivar in response to fungal infection. It is known that lipoxygenase (LOX) pathway products, such as jasmonates, are one of the major regulators of PPI gene expression (Christensen et al. 2015). In a previous study, we have reported a differential LOX activation in response to *A. parasiticus* infection using the same cultivar studied here (Muller et al. 2015). In both cultivars we observed an early response of LOX activity to fungal infection. However, a different composition of LOX enzyme driven by a differential co-expression of three *LOX genes* was found between cultivars. In these contexts, unraveling this network will challenge the understanding of the bases of peanut seed resistance to *Aspergillus spp.* infection and aflatoxin contamination.

ACKNOWLEDGEMENTS

V.M. is a recipient of a fellowship of Consejo Nacional de Investigaciones Científicas y Técnicas (CONICET), Argentina. V.A., F.C., G.B. and R.A. are members of Consejo Nacional de Investigaciones Científicas y Técnicas (Argentina). This work was partially financed by Instituto Nacional de Tecnología Agropecuaria (INTA), CONICET, Agencia Nacional de Promoción Científica y Tecnológica (ANPCyT) and Secretaria de Ciencia y Tecnología (SeCyT), UNC. We thank Carolina Mosconi, for linguistic revision of the manuscript.

LITERATURE CITED

Asis, R., Barrionuevo, D.L., Giorda, L.M.; Nores, M.L., and Aldao, M.A. 2005. Aflatoxin Production in six peanut (*Arachis hypogaea L.*) genotypes infected with *Aspergillus flavus* and *A. parasiticus*, isolated from peanut production areas of Cordoba, Argentina. J. Agric. Food Chem. 53: 9274−9280.

Asis, R., Muller, V., Barrionuevo, D.L., Araujo, S.A., Aldao, M.A. 2009. Analysis of protease activity in Aspergillus flavus and A. parasiticus on peanut seed infection and aflatoxin contamination. Eur. J. Plant Pathol. 124: 391-403.

Birk, Y. 1985. The bowman-birk inhibitor. trypsin- and chymotrypsin-inhibitor from soybeans. Int. J. Pept. Protein Res. 25: 113-131.

Boateng, J.A., Viquez, O.M., Konan, K.N., and Dodo, H.W. 2005. Screening of a peanut (arachis hypogaea L.) cDNA library to isolate a bowman-birk trypsin inhibitor clone. J. Agric. Food Chem. 53: 2028-2031.

Carrillo, L., Herrero, I., Cambra, I., Sánchez-Monge, R., Diaz, I., and Martinez, M. 2011. Differential in vitro and in vivo effect of barley cysteine and serine protease inhibitors on phytopathogenic microorganisms. Plant Physiol. Biochem. 49: 1191-1200.

Chen, Z.Y., Brown, R.L., Lax, A.R., Cleveland, T.E. and Russin, J.S. 1999. A. Inhibition of plant-pathogenic fungi by a corn trypsin inhibitor overexpressed in Escherichia coli. Appl. Environ. Microbiol. 65: 1320-1324.

Chen, Z.Y., Brown, L.R., Guo, B.Z., Menkir, A., and Cleveland, T.E. 2009. Identifying aflatoxin resistance related proteins/genes through proteomics and RNAi gene silencing. Peanut Sci. 36: 35-41.

Christensen SA, Huffaker A, Kaplan F, Sims J, Ziemann S, and Doehlemann G. 2015. Maize death acids, 9-lipoxygenase–derived cyclopente(a)nones, display activity as cytotoxic phytoalexins and transcriptional mediators. Proc. Natl. Acad. Sci. 112: 11407–11412.

Guo, B., Chen, X., Dang, P., Scully, B.T., Liang, X., Holbrook, C.C.,Yu, J., and Culbreath, A.K. 2008. Peanut gene expression profiling in developing seeds at different reproduction stages during aspergillus parasiticus infection. BMC Dev. Biol. 8.

Hörger, A.C., and van der Hoorn, R.A.L. 2013. The structural basis of specific protease-inhibitor interactions at the plant-pathogen interface. Curr. Opin. Struct. Biol. 23: 842-850.

InfoStat 2002. Grupo InfoStat Profesional. Facultad de Ciencias Agropecuarias, Universidad Nacional de Córdoba, Argentina

Jashni, M.K., Mehrabi, R., Collemare, J., Mesarich, C.H., and de Wit, P.J.G.M. 2015. The battle in the apoplast: Further insights into the roles of proteases and their inhibitors in plant–pathogen interactions. Front. Plant Sci. 6.

Joshi, B.N.; Sainani, M.N.; Bastawade, K.B.; Gupta, V.S. and Ranjekar, P.K. 1998. Cysteine protease inhibitor from pearl millet: a new class of antifungal protein. Biochem. Biophys. Res. Commun. 246: 382-387.

Kouzuma, Y.H., Inanaga, H., Doi-Kawano, K., Yamasaki, N, and Kimura, M. 2000. Molecular cloning and functional expression of cDNA encoding the cysteine proteinase inhibitor with three cystatin domains from sunflower seeds. J. Biochem. 128:161-166.

Lopes, J.L.S., Valadares, N.F., Moraes, D.I., Rosa, J.C., Araújo, H.S.S., and Beltramini, L.M. 2009. Physico-chemical and antifungal properties of protease inhibitors from acacia plumosa. Phytochemistry 70: 871-879.

Luo, M., Dang, P.; Guo, B.Z., He, G., Holbrook, C.C., Bausher, M.G. and Lee, R.D. 2005. Generation of expressed sequence tags (ESTs) for gene discovery and marker development in cultivated peanut. Crop Sci. 45: 346–353.

Luo, M., Liang, X.Q., Dang, P., Holbrook, C.C., Bausher, M.G., Lee, R.D., and Guo, B.Z. 2005. Microarray-based screening of differentially expressed genes in peanut in response to *Aspergillus parasiticus* infection and drought stress. Plant Sci. 169: 695-703.

Mosolov, V.V., and Valueva, T.A. 2005. Proteinase inhibitors and their function in plants: A review. Appl. Biochem. Microbiol. 41: 227-246.

Norioka, S.O. 1983. Amino acid sequencias of trypsin chymotrypsin inhibitors (AI, AII, BI, BII, BIII) from peanut (*Arachis hypogaea*):a discussion on the molecular evolution of legumes Bowman-Birk Type inhibitors. J. Biochem. 94: 589-599.

Park, K. S.; Cheong, J. J.; Lee, S. J.; Suh, M. C. and Choi, D. 2000. A novel proteinase inhibitor gene transiently induced by tobacco mosaic virus infection. Biochim Biophys Acta 1492: 509-12.

Roberts, W., and Selitrennikoff, C. P. 1990. Zeamatin, an antifungal protein from maize with membrane-permeabiliziting activity. J. Gen. Microbiol. 136: 1771-1778.

Schägger, H. 2006. Tricine-SDS-PAGE. Nat. Protoc. 1: 16-22.

Vernekar, J. V. G.; deshpande, M. S. 1999. Alkaline protease inhibitor: a novel class of antifungal proteins against phytopathogenic fungi. Biochem. Biophys. Res. Commun. 262: 702-707.

Wang, Z., Yan, S., Liu, C., Chen, F., and Wang, T. 2012. Proteomic analysis reveals an aflatoxin-triggered immune response in cotyledons of *Arachis hypogaea* infected with *Aspergillus flavus*. J. Proteome. Res. 11: 2739-2753.

Wang, H. X., & Ng, T. B. 2006. Concurrent isolation of a Kunitz-type trypsin inhibitor with antifungal activity and a novel lectin from pseudostellaria heterophylla roots. Biochem. Biophys. Res. Commun. 342: 349-353.

Yarullina, L. G., Akhatova, A. R., and Kasimova, R. I. 2016. Hydrolytic enzymes and their proteinaceous inhibitors in regulation of plant–pathogen interactions. Russ. J. Plant Physiol. 63: 193-203.

Table 1- Trypsin inhibitor units (TIU) activity of proteins precipitated at different acetone percentages starting from peanut seed extract of infected seeds of PI337394 and Florman cultivar. TIU is expressed per µg of protein. (*) means significant differences between acetone treatment.

% (v/v) Acetone	Peanut Cultivars	
	PI337394	Florman
30	4.81±0.03	0.32±0.21
70	50.66±2.23*	32.41±4.21*

Table 2- Protein identification by LC–MALDI TOF/TOF of Anionic exchange chromatography fractions.

Anion Exchange									
Spot Number	Cultivar	NCBI acc. no.	Uni Prot No.	MW (kDa)/pI (theoretical)	MW(kDa)/pI (observed)	identified peptides	MASCOT Score	sequence coverage	Protein
1	R	ES721458	gi|2827080	16.32/8.56	25.76/7.47	5	423	61	malate dehydrogenase
2	R	ES711412	gi| 77540216	23.59/7.14	23.91/7.11	4	251	38	triosephosphate isomerase
3	R	ES717793	gi|15221116	25.34/5.09	25.15/6.79	3	256	33	lactoylglutathione lyase-like protein
4	R	GO328251	gi| 211906514	29.23/9.29	25.46/6.30	4	211	25	lactoylglutathione lyase
5	R	GO333190	gi| 351720955	25.86/5.49	22.37/5.44	5	309	47	glutathione-S-transferase
6	R	JK157460		18.36/4.89	27.00/5.46	5	331	51	unknown
7	R	ES761053	GI:18143656	20.71/6.78	16.82/5.44	2	164	14	Kunitz trypsin inhibitor p20
8	R	EE124471	gi|145904610|	29.29/5.91	16.82/5.71	5	112	32	Ara h 8 allergen isoform
9	R and S	EE125497	gi|71040665	26.64/6.04	15.58/5.94	3	126	24	Cu-Zn superoxide dismutase
10	R	EE125497	gi|71040665	26.64/6.04	15.58/6.21	5	203	34	Cu-Zn superoxide dismutase
11	R		gi|71040665	15.09/5.27	13.11/6.57	3	85	44	Cu-Zn superoxide dismutase
12	R	EY396114	gi|255540625|	12.75/7.79	9.41/7.52	1	122	29	glutaredoxin-like protein
13	S	ES705001	gi|1942899	22.98/5.32	23.71/5.03	13	342	85	Chain A, Peanut Lectin
14	S	ES705001	gi|1942899	22.98/5.32	23.71/5.21	14	321	86	Chain A, Peanut Lectin
15	S	EG529656	gi|1942899	21.58/8.73	11.28/5.89	3	98	31	Peanut Lectin
16	S	GO333162	gi|2827080	22.58/10	27.22/7.06	9	256	52	malate dehydrogenase
17	S	EG357735	XP_002525645.1	31.72/7.71	29.46/7.74	5	156	27	Epidermis-specific secreted glycoprotein EP1
18	S	JK209541	emb|CAA61158.1|	20.11/9.22	29.46/8.55	4	263	39	glycoprotein EP1

Table 3- Protein identification by LC–MALDI TOF/TOF of Gel permeation chromatography fractions

Gel Permeation									
Spot Number	Cultivar	NCBI acc. no.	Uni Prot No.	MW (kDa)/pI (theoretical)	MW(kDa)/pI (observed)	identified peptides	MASCOT Score	sequence coverage	Protein
1	R and S		gi|351206	6736/ 7.53	5251/9.125	4	169	86	inhibitor,BIII trypsin chymotrypsin
2	R and S		gi|351443	6965/ 6.67	5487/7.37	3	106	74	inhibitor BI, protease
3	R		gi|213868275		5251/7.11	2	210		Ubiquitin
4	R	EE124396		14313/8.48	8024/7.02	5	165	60	similar to glutaredoxin
5	R and S		gi|33090235	8698/5.07	7232/5.75	5	94	100	Bowman-Birk trypsin inhibitor A-I
6	R		gi|124020	7628/5.08	8421/4.57	4	121	88	Bowman-Birk type proteinase inhibitor A-II
7	R		gi|145904610	16402/5.07	17533/5.01	4	187	53	Ara h 8 allergen isoform
8	R		gi|145904610	16402/5.07	17930/5.19	4	175	53	Ara h 8 allergen isoform
9	R and S		gi|71040665	15089/5.27	15552/5.67	3	107	38	Cu-Zn superoxide dismutase
10	R and S		gi|53830013	10018/6.73	12382/5.75	3	124	69	PR protein 4A
11	S	ES703500		20035/9.23	5647/7.11	3	123	21	Acyl-CoA-binding protein
12	S		gi|1942899	25174/4.99	25457/4.84	6	322	42	Chain A, Peanut Lectin
13	S		gi|1942899	25174/4.99	25457/4.58	5	337	45	Chain A, Peanut Lectin

FIGURE LEGENDS

Fig. 1 Purification of plant protease inhibitors of infected peanut seeds by Anion-exchange chromatography. A) Chromatograms of seed extracts from Floman (gray line) and PI337394 cultivars (black line), elution fractions inside ellipses show PPI activity. B) PPI activity of pooled fractions, expressed as Trypsin inhibitor units/ml. C) Reverse zymography of pooled fraction 17-18-19 of both cultivars.

Fig. 2 Purification of plant protease inhibitors of infected peanut seeds by gel permeation chromatography. A) Chromatograms of seed extracts from Florman (gray line) and PI337394 cultivars (black line), elution fractions inside the ellipse show PPI activity. B) PPI activity of pooled fractions 14-15-16, expressed as Trypsin inhibitor units. C) Reverse zymography of pooled fraction 14-15-16 of both cultivars.

Fig. 3 Seed protein profiles of AEC elution fractions of A) PI337394 and B) Florman cultivars resolved in 2D-electrophoresis. Seed proteins were separated on 7 cm IPG (pH 3–10) strips in the first dimension followed by tris-tricine SDS-PAGE (16 %).

Fig. 4 Seed protein profiles of GPC elution fractions of PI337394 and Florman cultivars resolved in 2D-electrophoresis. Seed proteins were separated on 7 cm IPG (pH 3–10) strips in the first dimension followed by tris-tricine SDS-PAGE (16 %).

Fig. 5 Antifungal assay of AEC 17-19 fraction of PI337394 cultivar. A) Microscopic image (40x) of *A. parasiticus* mycelium growth in Muller Hinton with 20 mM tris-HCl buffer pH 8.9 / 0.5 M NaCl after 24 h of incubation at 37C. B) Microscopic image (40x) of *A. parasiticus* mycelium growth in Muller Hinton with fraction AEC 17-19 (20 µg of protein).

Fig. 6 Zymography of *A. parasiticus* extracellular proteases: A) proteases incubated in the absence of inhibitors. B) proteases incubated with commercial inhibitors mix (EDTA, PMSF, Iodoacetamide). C) proteases incubated with peanut PPI obtained by precipitation with acetone 70% (v/v).

Fig. 7 Visual infection, Trypsin inhibitory unit activity (TIU) and qRT-PCR analysis of *BBTI and KPI* genes in PI 337394 cultivar (black bars) and Florman INTA cultivar (gray bars). TIU and gene expression are represented as fold change of infected

seeds with respect to the average value of control seeds corresponding to the same time after inoculation. Values between 1 and -1 mean do not change with respect to those of the control.

A) % of infected seeds. **B)** Fold change of *TIU.* **C)** Fold change of *BBTI*. **D)** Fold change of *KPI.*

E-XTRA FIGURE CAPTIONS

Supplementary Table 1 Selected genes, primer sets and amplicon characteristics for qPCR

Supplementary Fig. S1 Peanut seeds after 48 hs of *A. parasiticus* inoculation. A) seeds of PI337394 cultivar, B) seeds of Florman Cultivar. The pictures correspond to one of the four replicates made for PPI purification.

Supplementary Fig. S2 A) Nucleotide sequence of Kunitz *Arachis hypogaea* inhibitor. Bold letters showed the predicted open reading frame (ORF), **B)** Protein sequence translated from predicted ORF and **C)** Predicted Conserved domain of Kunitz inhibitors by NCBI's conserved domain database.

Supplementary Fig. S3 Comparison of peanut protease inhibitors with the aminoacid sequences of different plant protease inhibitors in a phylogenetic tree analysis. The tree was compiled using the on line Phylogeny.fr platform (http://www.phylogeny.fr/) that provides a phylogeny pipeline based on MUSCLE for multiple alignment, Gblocks for alignment curation, PhyML for phylogeny and finally TreeDyn for tree drawing. **A)** Comparison of peanut KPI with the aminoacid sequences of different plant kunitz inhibitor. The proteins mentioned in the tree were obtained from Merops database for I3 plant kunitz inhibitor family (http://merops.sanger.ac.uk/cgi-bin/famsum?family=I3). **B)**

Comparison of peanut BBTI with the aminoacid sequences of different plant BBTI. The proteins mentioned in the tree were obtained from Merops database for plant BBTI family (http://merops.sanger.ac.uk/inhibitors).

Supplementary Fig. S4 Sequence alignment of **A)** plant Kunitz inhibitor proteins and **B)** plant BBTI proteins. Characteristic residue of kunitz inhibitor are indicated by boxes, Red box show the cysteine residues, yellow box show the active site and blue box show the aminoacid necessary for the loop stabilization. Active sites of BBTI are indicated by red boxes.

Supplementary Fig. S5 *A. parasiticus* development in Mueller Hinton medium with GPC 14-16 fraction (20 µg of proteins) of both cultivars. After 24 hs of incubation, absorbance at 600 nm was determined in treatment and control (in absence of GPC fraction) and expressed as the absorbance relative to control.

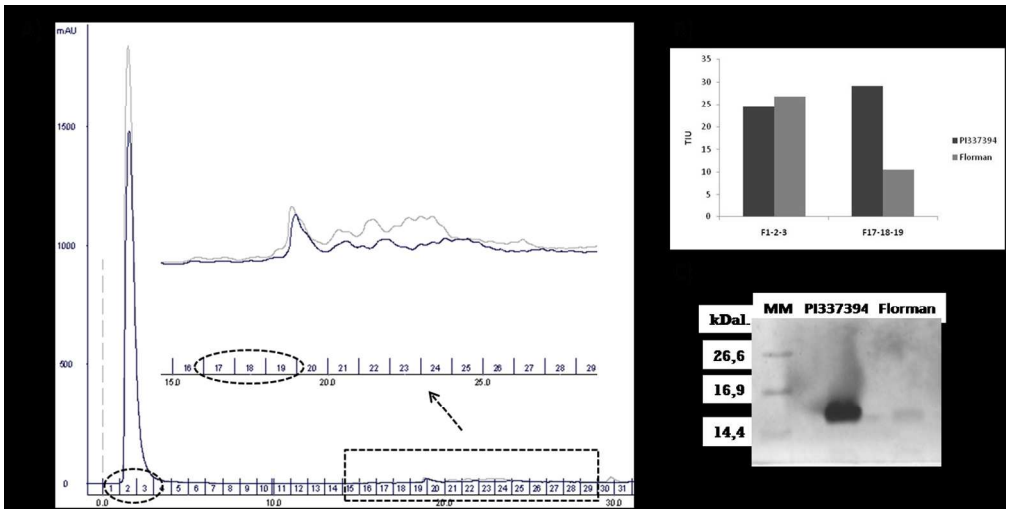

Fig. 1 Purification of plant protease inhibitors of infected peanut seeds by Anion-exchange chromatography. A) Chromatograms of seed extracts from Floman (gray line) and PI337394 cultivars (black line), elution fractions inside ellipses show PPI activity. B) PPI activity of pooled fractions, expressed as Trypsin inhibitor units/ml. C) Reverse zymography of pooled fraction 17-18-19 of both cultivars.
Fig. 1
253x127mm (150 x 150 DPI)

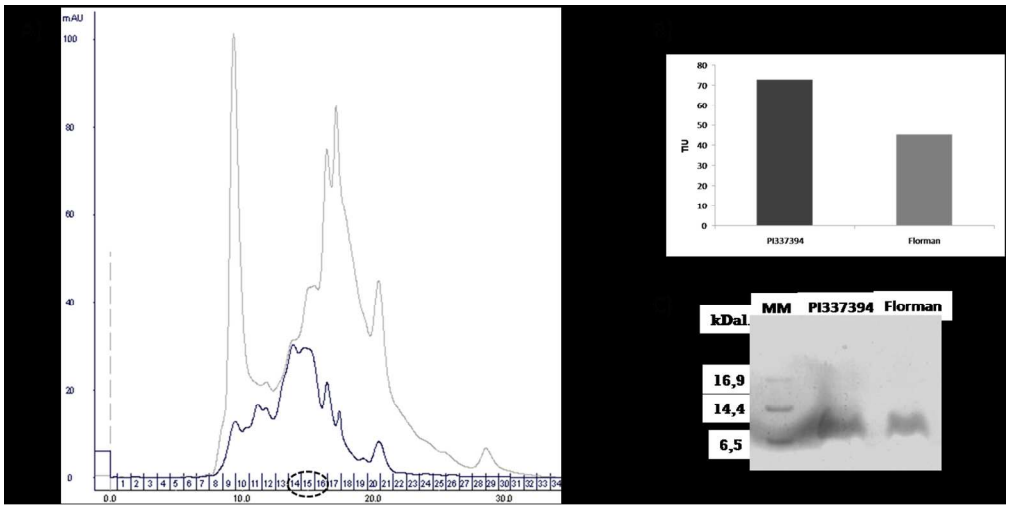

Fig. 2 Purification of plant protease inhibitors of infected peanut seeds by gel permeation chromatography. A) Chromatograms of seed extracts from Florman (gray line) and PI337394 cultivars (black line), elution fractions inside the ellipse show PPI activity. B) PPI activity of pooled fractions 14-15-16, expressed as Trypsin inhibitor units. C) Reverse zymography of pooled fraction 14-15-16 of both cultivars.
Fig. 2
251x125mm (150 x 150 DPI)

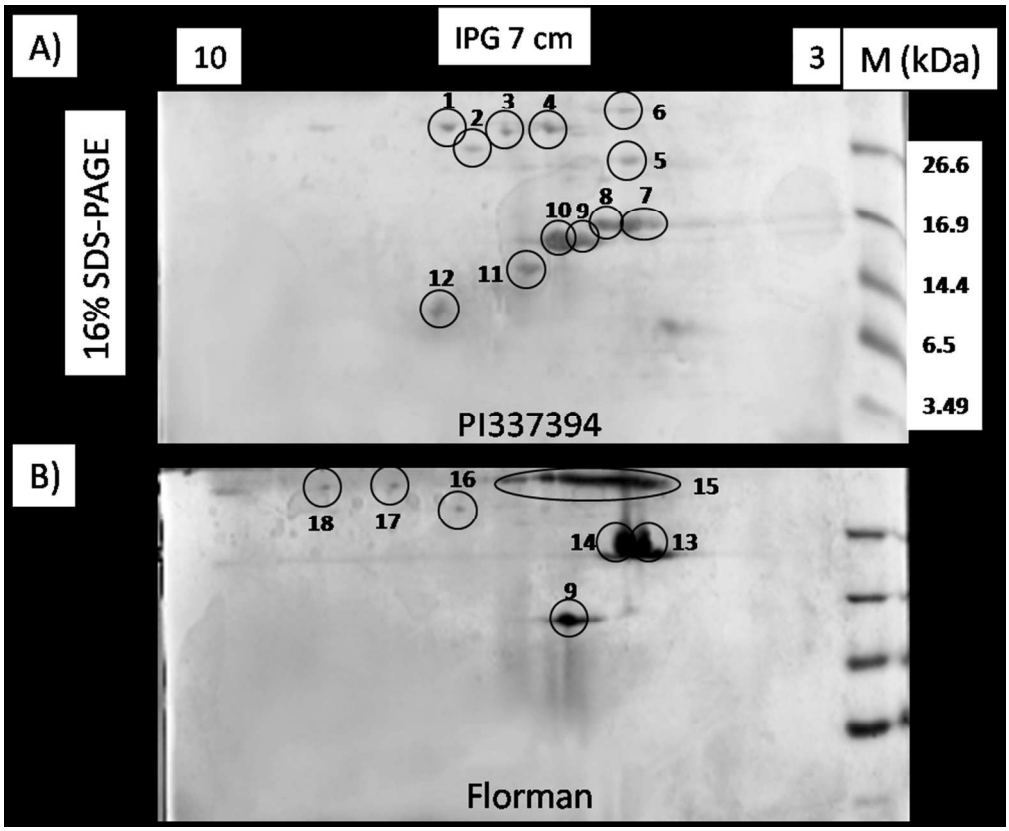

Fig. 3 Seed protein profiles of AEC elution fractions of A) PI337394 and B) Florman cultivars resolved in 2D-electrophoresis. Seed proteins were separated on 7 cm IPG (pH 3–10) strips in the first dimension followed by tris-tricine SDS-PAGE (16 %).

Fig. 3

168x138mm (150 x 150 DPI)

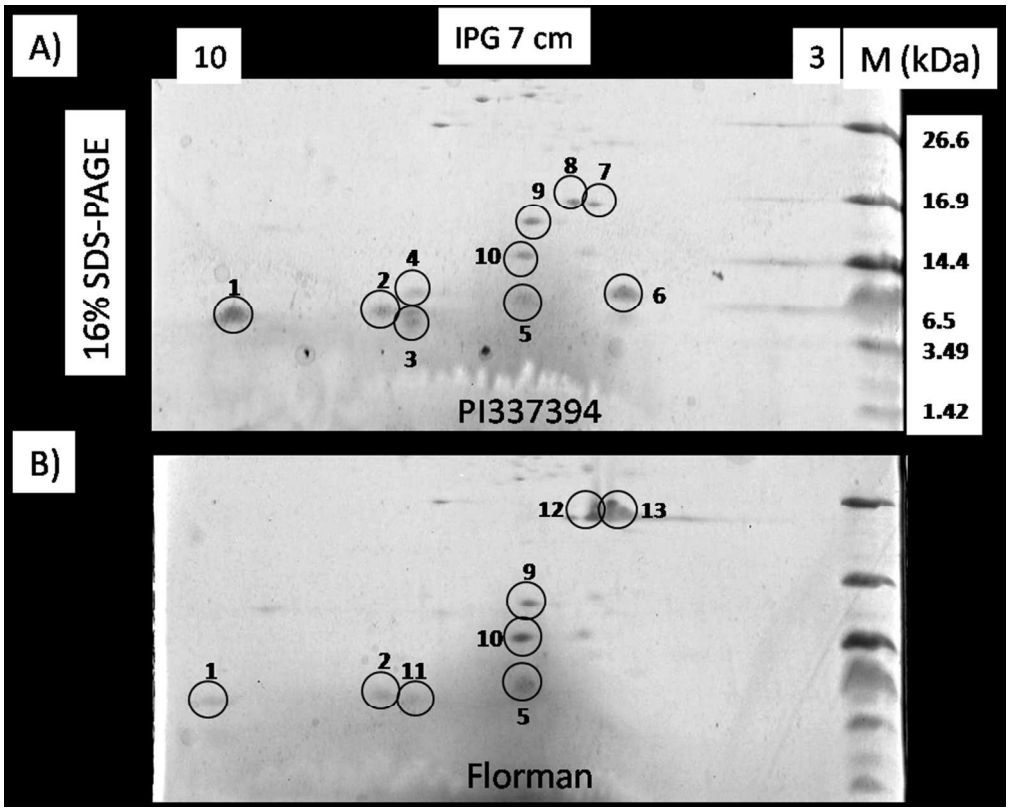

Fig. 4 Seed protein profiles of GPC elution fractions of PI337394 and Florman cultivars resolved in 2D-electrophoresis. Seed proteins were separated on 7 cm IPG (pH 3–10) strips in the first dimension followed by tris-tricine SDS-PAGE (16 %).
Fig. 4
168x134mm (150 x 150 DPI)

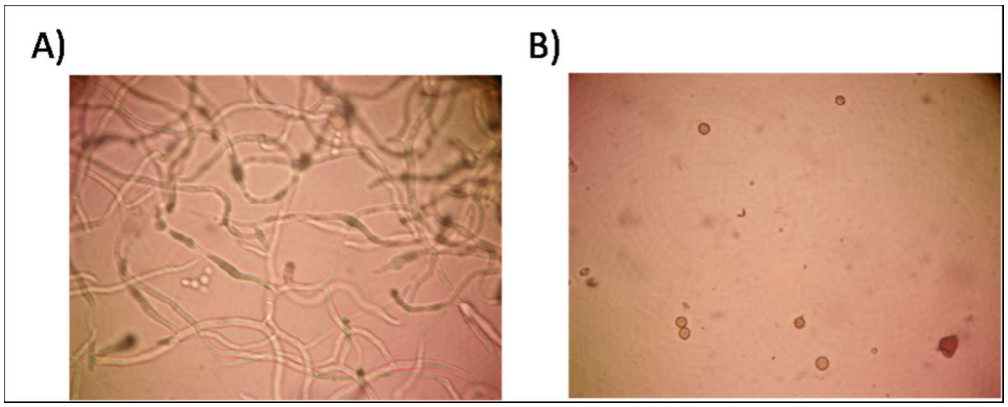

Fig. 5 Antifungal assay of AEC 17-19 fraction of PI337394 cultivar. A) Microscopic image (40x) of A. parasiticus mycelium growth in Muller Hinton with 20 mM tris-HCl buffer pH 8.9 / 0.5 M NaCl after 24 h of incubation at 37C. B) Microscopic image (40x) of A. parasiticus mycelium growth in Muller Hinton with fraction AEC 17-19 (20 µg of protein).
Fig. 5
230x91mm (104 x 104 DPI)

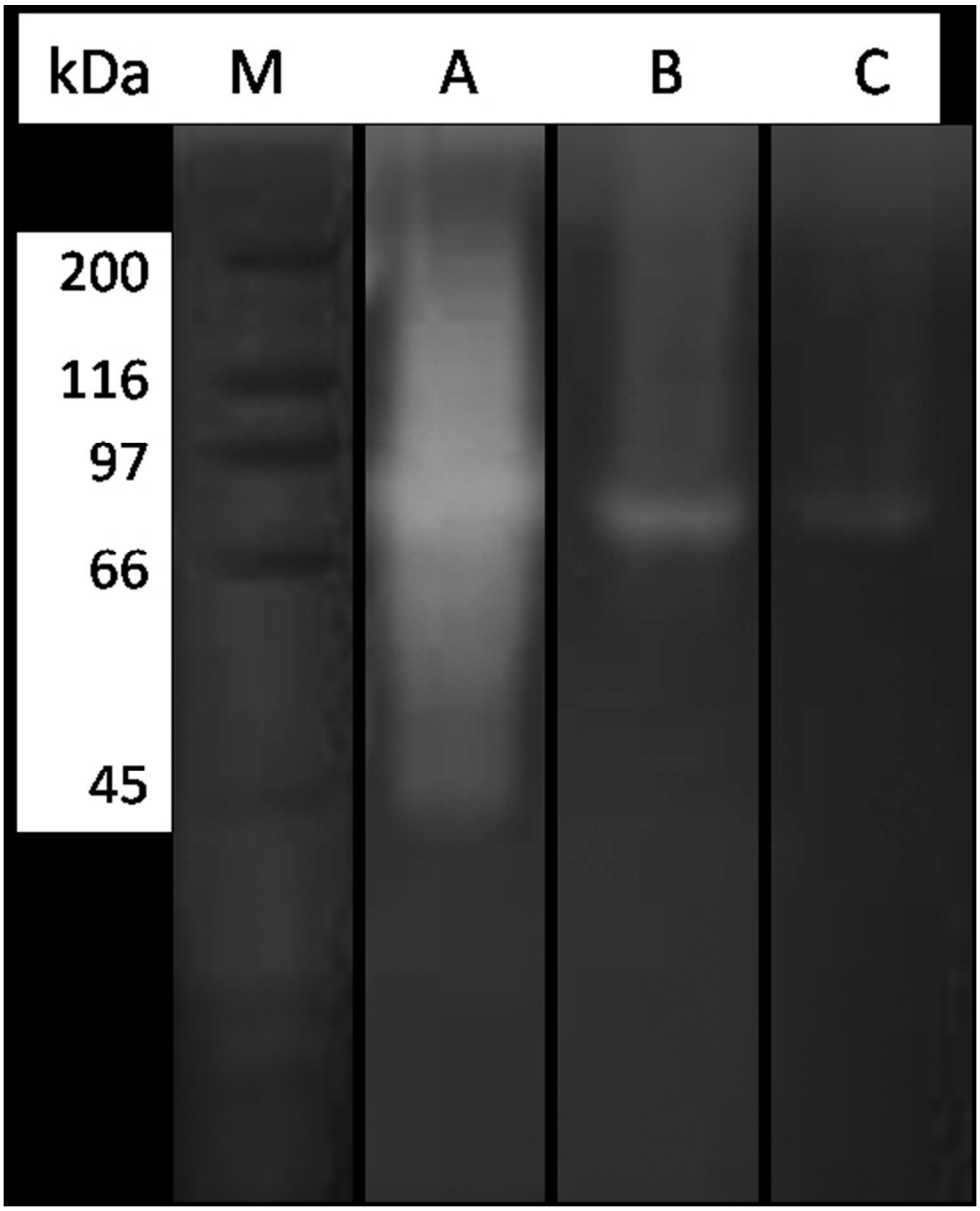

Fig. 6 Zymography of A. parasiticus extracellular proteases: A) proteases incubated in the absence of inhibitors. B) proteases incubated with commercial inhibitors mix (EDTA, PMSF, Iodoacetamide). C) proteases incubated with peanut PPI obtained by precipitation with acetone 70% (v/v).
Fig. 6
91x113mm (150 x 150 DPI)

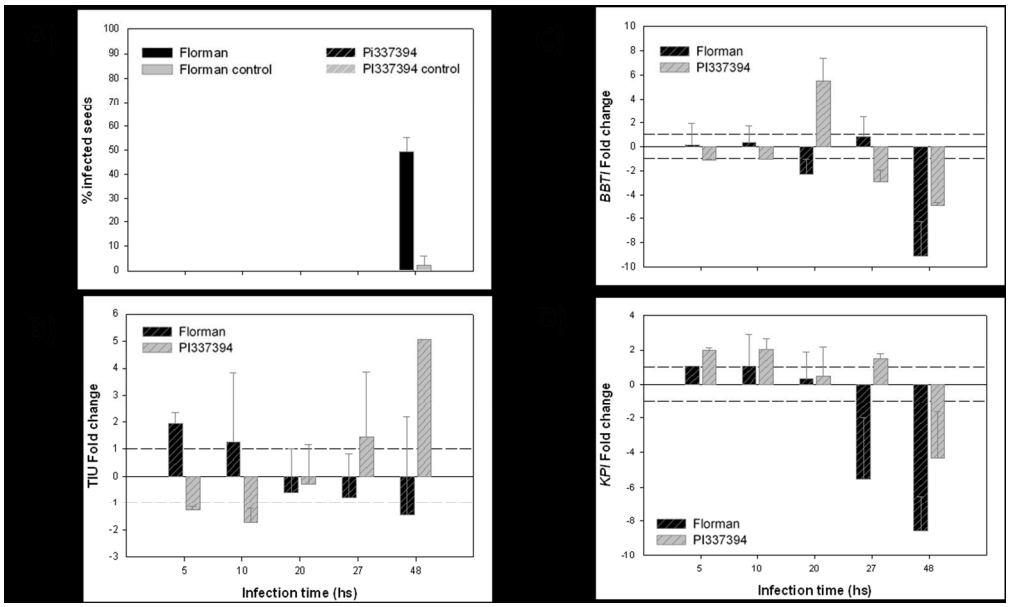

Fig. 7 Visual infection, Trypsin inhibitory unit activity (TIU) and qRT-PCR analysis of BBTI and KPI genes in PI 337394 cultivar (black bars) and Florman INTA cultivar (gray bars). TIU and gene expression are represented as fold change of infected seeds with respect to the average value of control seeds corresponding to the same time after inoculation. Values between 1 and -1 mean do not change with respect to those of the control.
A) % of infected seeds. B) Fold change of TIU. C) Fold change of BBTI. D) Fold change of KPI.

Fig. 7
204x121mm (150 x 150 DPI)

A) B)

Supp. Fig. 1 Peanut seeds after 48 hs of *A. parasiticus* inoculation. A) seeds of PI337394 cultivar, B) seeds of Florman Cultivar. The pictures correspond to one of the four replicates made for PPI purification.

A) >gi|149650070|gb|ES761053.1|ES761053 ISBL_4_E02_E003.g1 USDA-Tifton Peanut Library ISBL Arachis hypogaea cDNA clone ISBL004_E02_007 5', mRNA sequence.

AAATATATAAAAAAAA**ATGAAGGCTACAACCACCACCAATGTCTTCGCCATTTTCATTCTCTTTGCTTTCATTTCCA**
TCCACCTACCTTCTTTAGCCACGGCTGAGTTGGTCGACACAGACGGCAACCTTATCAAAAACGGCGGCTTATACT
TCATCCTCCCAGTTTTTCGAGGCAACGGCGGCGGAATAGGCCGAATATCAACCGGAAACGAAACGTGTCCACTA
ACCGTTGTCCAACAACGCTCCGAAGTGGACAACGGATCACCAATTATAATTTCATCTCCATTGAGAATCCCTTTTC
TCCGTGAAGGATTTCCTTTGGACCTGTCCTTTTCAGCTGTTCCTTTCTGTACTCCTACTCCTTCCAAGTGGACCCTC
GTTAAGGGTCTACTGGAAGGAGAAGGAGCCACGGTGAAACTCACCGGTTTTTACGAGAACGAGATACAGGGTT
GGTTTGAGATAAGGAAAACCTTGGATGCCTTTAAACTTACCTTCTGTGCTTCTTCAAATAATAATTGCATGGATA
TTGGGGTTAAACGTGATGATGAGGGAAATAGGCTTTTGGTTGCAACGGA

B) >Translation of ORF in reading frame 2 on the direct strand.

MKATTTTNVFAIFILFAFISIHLPSLATAELVDTDGNLIKNGGLYFILPVFRGNGGGIGRISTGNETCPLTVVQQRSEVDNG
SPIIISSPLRIPFLREGFPLDLSFSAVPFCTPTPSKWTLVKGLLEGEGATVKLTGFYENEIQGWFEIRKTLDAFKLTFCASSNN
NCMDIGVKRDDEGNRLLVAT

C)

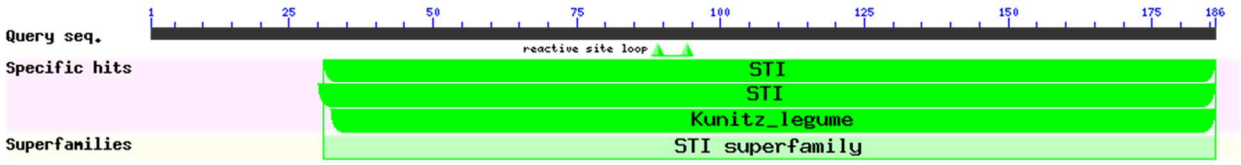

Supp. Fig. 2 A) Nucleotide sequence of Kunitz *Arachis hypogaea* inhibitor. Bold letters showed the predicted open reading frame (ORF), **B)** Protein sequence translated from predicted ORF and **C)** Predicted Conserved domain of Kunitz inhibitors by NCBI's conserved domain database.

A)

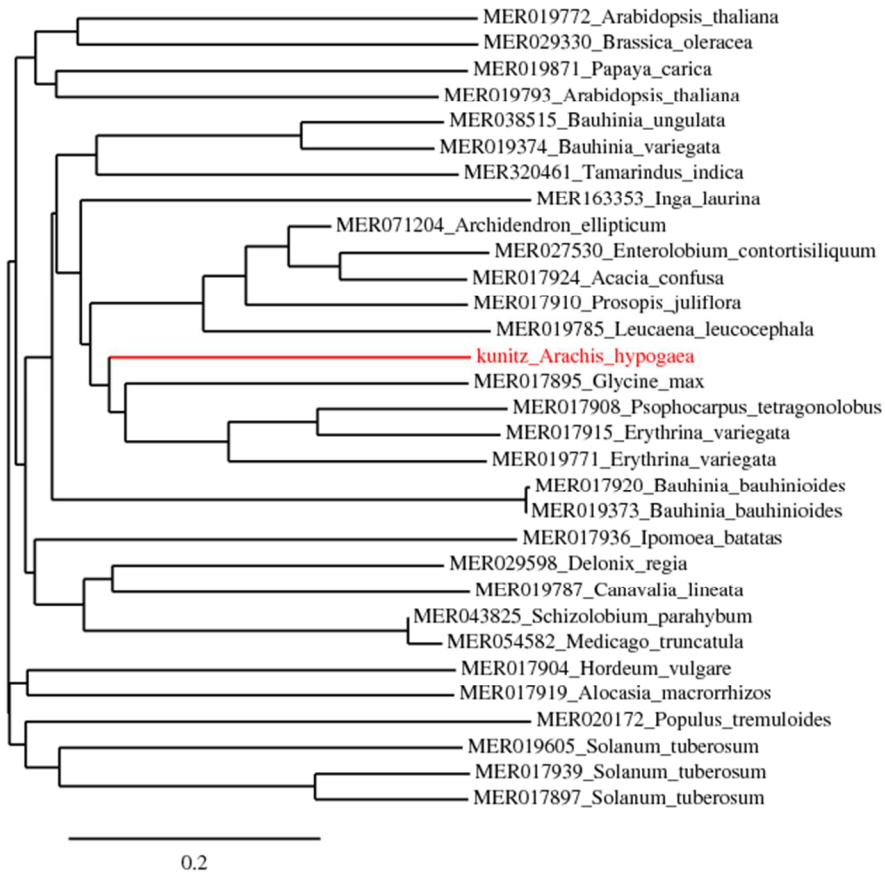
MER019772_Arabidopsis_thaliana
MER029330_Brassica_oleracea
MER019871_Papaya_carica
MER019793_Arabidopsis_thaliana
MER038515_Bauhinia_ungulata
MER019374_Bauhinia_variegata
MER320461_Tamarindus_indica
MER163353_Inga_laurina
MER071204_Archidendron_ellipticum
MER027530_Enterolobium_contortisiliquum
MER017924_Acacia_confusa
MER017910_Prosopis_juliflora
MER019785_Leucaena_leucocephala
kunitz_Arachis_hypogaea
MER017895_Glycine_max
MER017908_Psophocarpus_tetragonolobus
MER017915_Erythrina_variegata
MER019771_Erythrina_variegata
MER017920_Bauhinia_bauhinioides
MER019373_Bauhinia_bauhinioides
MER017936_Ipomoea_batatas
MER029598_Delonix_regia
MER019787_Canavalia_lineata
MER043825_Schizolobium_parahybum
MER054582_Medicago_truncatula
MER017904_Hordeum_vulgare
MER017919_Alocasia_macrorrhizos
MER020172_Populus_tremuloides
MER019605_Solanum_tuberosum
MER017939_Solanum_tuberosum
MER017897_Solanum_tuberosum
0.2

B)

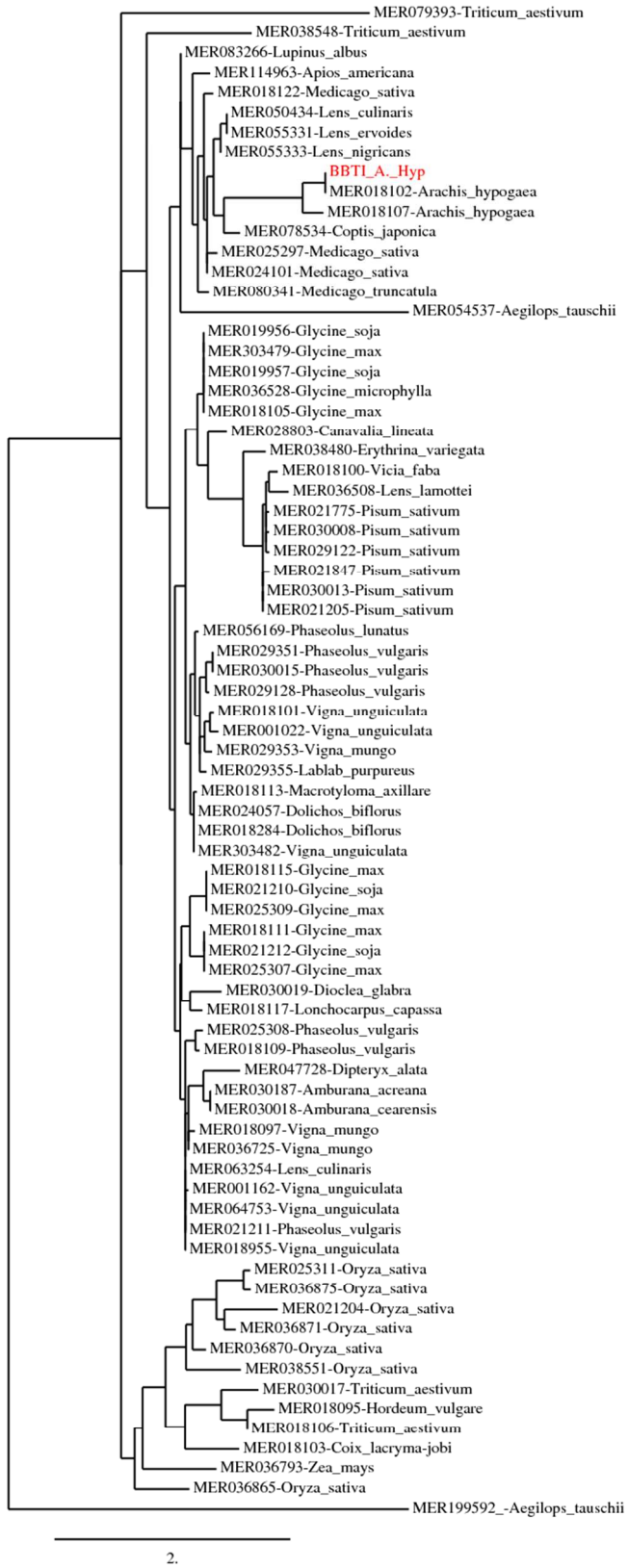
MER079393-Triticum_aestivum
MER038548-Triticum_aestivum
MER083266-Lupinus_albus
MER114963-Apios_americana
MER018122-Medicago_sativa
MER050434-Lens_culinaris
MER055331-Lens_ervoides
MER055333-Lens_nigricans
BBTI_A._Hyp
MER018102-Arachis_hypogaea
MER018107-Arachis_hypogaea
MER078534-Coptis_japonica
MER025297-Medicago_sativa
MER024101-Medicago_sativa
MER080341-Medicago_truncatula
MER054537-Aegilops_tauschii
MER019956-Glycine_soja
MER303479-Glycine_max
MER019957-Glycine_soja
MER036528-Glycine_microphylla
MER018105-Glycine_max
MER028803-Canavalia_lineata
MER038480-Erythrina_variegata
MER018100-Vicia_faba
MER036508-Lens_lamottei
MER021775-Pisum_sativum
MER030008-Pisum_sativum
MER029122-Pisum_sativum
MER021847-Pisum_sativum
MER030013-Pisum_sativum
MER021205-Pisum_sativum
MER056169-Phaseolus_lunatus
MER029351-Phaseolus_vulgaris
MER030015-Phaseolus_vulgaris
MER029128-Phaseolus_vulgaris
MER018101-Vigna_unguiculata
MER001022-Vigna_unguiculata
MER029353-Vigna_mungo
MER029355-Lablab_purpureus
MER018113-Macrotyloma_axillare
MER024057-Dolichos_biflorus
MER018284-Dolichos_biflorus
MER303482-Vigna_unguiculata
MER018115-Glycine_max
MER021210-Glycine_soja
MER025309-Glycine_max
MER018111-Glycine_max
MER021212-Glycine_soja
MER025307-Glycine_max
MER030019-Dioclea_glabra
MER018117-Lonchocarpus_capassa
MER025308-Phaseolus_vulgaris
MER018109-Phaseolus_vulgaris
MER047728-Dipteryx_alata
MER030187-Amburana_acreana
MER030018-Amburana_cearensis
MER018097-Vigna_mungo
MER036725-Vigna_mungo
MER063254-Lens_culinaris
MER001162-Vigna_unguiculata
MER064753-Vigna_unguiculata
MER021211-Phaseolus_vulgaris
MER018955-Vigna_unguiculata
MER025311-Oryza_sativa
MER036875-Oryza_sativa
MER021204-Oryza_sativa
MER036871-Oryza_sativa
MER036870-Oryza_sativa
MER038551-Oryza_sativa
MER030017-Triticum_aestivum
MER018095-Hordeum_vulgare
MER018106-Triticum_aestivum
MER018103-Coix_lacryma-jobi
MER036793-Zea_mays
MER036865-Oryza_sativa
MER199592_-Aegilops_tauschii
2.

Supp. Fig. 3 Comparison of peanut protease inhibitors with the aminoacid sequences of different plant protease inhibitors in a phylogenetic tree analysis. The tree was compiled using the on line Phylogeny.fr platform (http://www.phylogeny.fr/) that provides a phylogeny pipeline based on MUSCLE for multiple alignment, Gblocks for alignment curation, PhyML for phylogeny and finally TreeDyn for tree drawing. A) Comparison of peanut KPI with the aminoacid sequences of different plant kunitz inhibitor. The proteins mentioned in the tree were obtained from Merops database for I3 plant kunitz inhibitor family (http://merops.sanger.ac.uk/cgi-bin/famsum?family=I3). B) Comparison of peanut BBTI with the aminoacid sequences of different plant BBTI. The proteins mentioned in the tree were obtained from Merops database for plant BBTI family (http://merops.sanger.ac.uk/inhibitors).

A)

B)

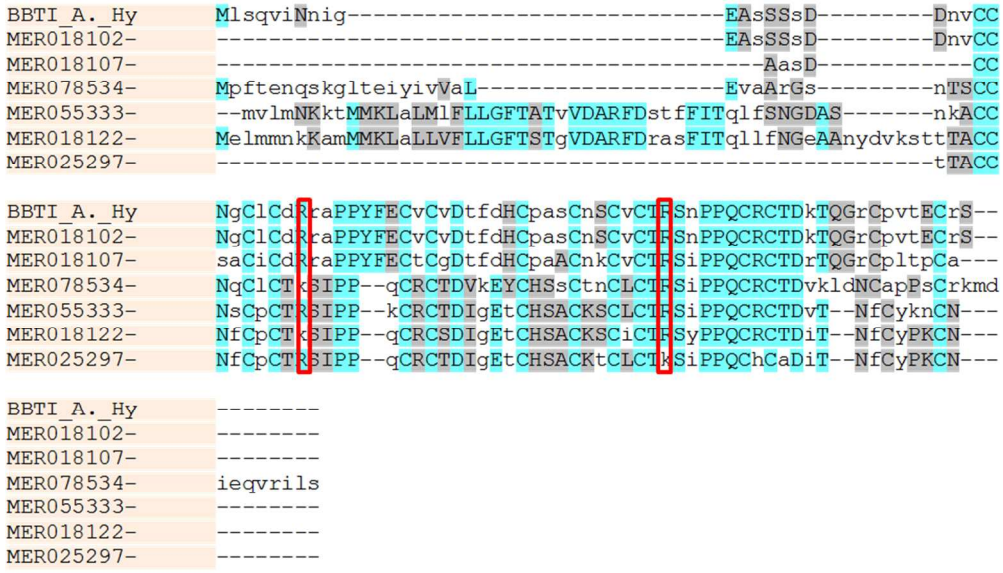

Supp. Fig. 4 Sequence alignment of **A)** plant Kunitz inhibitor proteins and **B)** plant BBTI proteins.

Characteristic residue of kunitz inhibitor are indicated by boxes, Red box show the cysteine

residues, yellow box show the active site and blue box show the aminoacid necessary for the loop stabilization. Active sites of BBTI are indicated by red boxes.

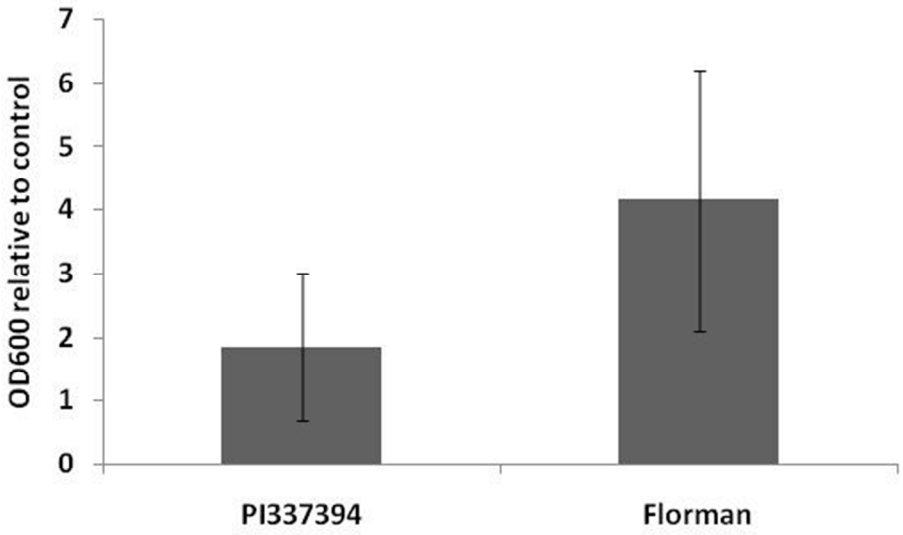

Supp. Fig. 5 *A. parasiticus* development in Mueller Hinton medium with GPC 14-16 fraction (20 µg of proteins) of both cultivars. After 24 hs of incubation, absorbance at 600 nm was determined in treatment and control (in absence of GPC fraction) and expressed as the absorbance relative to control.

Supp. Table 1 Selected genes, primer sets and amplicon characteristics for qPCR

Gene symbol	NCBI Accession number	Forward Primer sequence [5'-3']	Reverse Primer sequence [5'-3']	Amplicon lengh (bp)	Melting Temperature (°C)
H3	AY378165	ACAGCTCGCAAATCAACCG	GCGGCTTCTTCACTCCACC	100	83,79
BBTI	AY330200.1	TTGTGTTGACACGTTCGATCATT	TGGAGGATTAGACCTTGTGCAA	70	56,1
KTI	ES761053	CGACACAGACGGCAACCTT	CCGCCGTTGCCTCGAAAA	72	58